JOURNAL OF THE MECHANICAL BEHAVIOR OF BIOMEDICAL MATERIALS 32 (2014) 279–286

Available online at www.sciencedirect.com

ScienceDirect

www.elsevier.com/locate/jmbbm

Research Paper

Mechanical behavior of transparent nanofibrillar cellulose–chitosan nanocomposite films in dry and wet conditions

Tongfei Wu[a,b,c], *Ramin Farnood*[b], *Kevin O'Kelly*[c], *Biqiong Chen*[a,*]

[a]*Department of Materials Science and Engineering, University of Sheffield, Mappin Street, Sheffield S1 3JD, UK*
[b]*Department of Chemical Engineering and Applied Chemistry, University of Toronto, 200 College Street, Toronto, ON, Canada M5S 3E5*
[c]*Department of Mechanical and Manufacturing Engineering, Trinity College Dublin, College Green, Dublin 2, Ireland*

ARTICLE INFO

Article history:
Received 23 September 2013
Received in revised form
16 January 2014
Accepted 18 January 2014
Available online 27 January 2014

Keywords:
Chitosan
Nanofibrillar cellulose
Nanocomposites
Mechanical properties

ABSTRACT

Transparent, biocompatible and biodegradable chitosan (CS) nanocomposite films reinforced with nanofibrillar cellulose (NFC) were prepared by solution casting. The effects of NFC content on the mechanical properties in dry and wet conditions were investigated. The incorporation of NFC significantly enhanced the mechanical properties, especially in wet conditions. The ultimate tensile strength and Young's modulus of chitosan were improved by 12 times and 30 times, respectively, for the nanocomposite containing 32 wt% of NFC in wet conditions. The mechanism of the remarkable reinforcements was studied by analyzing the swelling behavior of NFC–CS nanocomposites. The mechanical properties of wet NFC–CS nanocomposite films matched well with those of human skin, which demonstrate potential for uses as artificial skin and wound dressings.

1. Introduction

Polymers from biomass resources (e.g., polysaccharides, silk, lignin and gelatin) have attracted significant attention from researchers with expertise in diverse areas, due to the predictable scarcity of fossil resources and the environmental problems (Williams and Hillmyer, 2008). Polysaccharides (e.g., chitosan, cellulose and starch) are an important class of biological polymers. They have been of increasing interest as polymeric renewable materials in the last few decades, not only because they are naturally abundant, eco-friendly and sustainable, but also because of their interesting properties (Fernandes et al., 2009).

Chitosan (CS) is a linear polysaccharide containing glucosamine and aminated glucosamine derived from chitin by N-deacetylation (Muzzarelli, 2009; Rinaudo, 2006). It is one of the most widely investigated and used structural polymers due to its excellent film-forming ability, biocompatibility, biodegradability and antimicrobial activity (Dash et al., 2011; Khor and Lim, 2003; Pillai et al., 2009). Chitosan can be applied in various fields for scientific and industrial interest, such as waste treatment, packaging, food processing and medicine (Crini and Badot, 2008; Krajewska, 2004; Ravi Kumar, 2000; Şenel and McClure, 2004; Shahidi et al., 1999). The medical applications include novel drug delivery, wound healing and tissue engineering (Agnihotri et al., 2004; Jayakumar et al., 2010; Kim

*Corresponding author. Tel.: +44 114 222 5958; fax: +44 114 222 5943.
E-mail address: biqiong.chen@sheffield.ac.uk (B. Chen).

1751-6161/$ - see front matter © 2014 Elsevier Ltd. All rights reserved.
http://dx.doi.org/10.1016/j.jmbbm.2014.01.014

et al., 2008; Sashiwa and Aiba, 2004). More recently, the incorporation of nano-fillers, such as clay (Wang et al., 2005), graphene oxide (Pan et al., 2011), carbon nanotube (Azeez et al., 2013), hydroxyapatite (Verma et al., 2008) and metal nanoparticles (Huang et al., 2004) into chitosan has been widely investigated to obtain chitosan hybrids with superior mechanical and barrier properties, while remaining high transparency.

Nanofibrillar cellulose (NFC) consists of elementary cellulose nanofibrils or their bundles, having a high aspect ratio and a large specific surface area (Siró and Plackett, 2010). The diameter of NFC lies typically in the range of 5–50 nm, while the length of the fibers can exceed 1 μm (Herrick et al., 1983). NFC has a high elastic modulus (~140 GPa) (Nishiyama, 2009), a high tensile strength (2–3 GPa) (Matsuo et al., 1990; Sakurada et al., 1962), as well as a low thermal expansion coefficient (0.1 ppm/K) (Nishino et al., 2004; Shimazaki et al., 2007). NFC is also non-cytotoxic and non-genotoxic (Pitkänen et al., 2010). NFC is believed to be a promising material allowing technical solutions by a green and sustainable means. NFC has been proposed as rheology modifiers due to the long and entangled fibrils (Pääkkö et al., 2007), as materials for functional aerogels (Olsson et al., 2010) and as matrix materials in transparent paper, packaging, coatings and pharmaceutical products (Henriksson et al., 2008; Herrick et al., 1983; Nogi et al., 2009; Turbak et al., 1983). It is also used as an attractive component for reinforcement of polymers (Baheti and Militky, 2013; Dahman and Oktem, 2012; Wu et al., 2007).

Chitosan nanocomposites filled by NFC are full-polysaccharide nanocomposites, which are a relatively new class of materials (Hassan et al., 2011, 2012; Li et al., 2009; Nakagaito and Yano, 2004, 2005; Tsourounaki et al., 2008). NFC–CS nanocomposite films were reported of high light transmittance and good mechanical properties (Fernandes et al., 2010, 2009). Chitosan and cellulose have similar chemical structures and are expected to possess excellent biocompatibility and biodegradability when compounded into hybrids. The mechanical and other physical properties of NFC–CS films are also expected to satisfy the basic requirements for biomedical applications, having promising potential in the fields of transparent edible films and coatings, artificial skin and wound dressings. However, the wet mechanical behavior of NFC–CS nanocomposites, which are more important in practical applications in artificial skin and wound dressings than the dry state, have not been reported to our knowledge. It was well known that one critical drawback regarding the use of chitosan as a structural polymer is its poor mechanical properties in wet conditions (Li et al., 2007; Oh and Hwang, 2013). NFC is expected to be able to reinforce chitosan in wet conditions. In this work, we prepared highly transparent NFC–CS nanocomposite films, investigated the swelling behavior and mechanical properties of NFC–CS nanocomposites at dry and wet conditions, and examined the comparability of their wet mechanical behavior with human skins.

2. Materials and methods

2.1. Materials

Chitosan with a medium molecular weight (75–85% deacetylated) and acetic acid were purchased from Sigma-Aldrich. Nanofibrillar cellulose aqueous suspension (2 wt%) was received from Professor Mohini Sain's group in the Centre for Biocomposites and Biomaterials Processing, Faculty of Forestry, University of Toronto.

2.2. Fabrication of NFC–CS nanocomposites

Chitosan solution (1 wt%) was prepared by mixing 1 g of CS, 1 g of acetic acid and 98 g of distilled water for 4 h under stirring and purified by centrifugation. Subsequently, a desired amount of nanofibrillar cellulose suspension was added into the CS solution. The mixture was then stirred at 1000 rpm for 6 h, followed by sonication for 10 min to remove the bubbles. After that, the NFC–CS suspension was poured into a plastic dish and placed in a fume hood at room temperature to allow water to evaporate to form a film, followed by drying in a vacuum oven at 50 °C for 24 h. The thicknesses of final films were between 0.10 and 0.15 mm. The as-cast films containing 0, 1, 2, 4, 8, 16 and 32 wt% of NFC were prepared and were designated as CS, CS1, CS2, CS4, CS8, CS16 and CS32, respectively.

2.3. Characterization and measurements

Ultraviolet–visible spectrometry (UV–vis, Varian Cary 50 Bio Spectrophotometer) was used to measure the light transmittance of as-cast NFC–CS films in the range of 215–800 nm.

Scanning electron microscopy (SEM) micrographs of NFC and the cross section of CS32 were obtained on an Inspect F (FEI) operating at 10 kV. Prior to SEM observations, samples were sputter-coated with gold using an SPI sputter coater for enhanced conductivity.

The swelling degree of the NFC–CS samples was calculated by measuring the weight before immersion (W_{dry}) and the weight after immersion (W_{wet}) in distilled water, according to Eq. (1) (Lagarón and Fendler, 2009; Mendez et al., 2011). To minimize the error in measuring the water uptake, once the wet samples were taken out of water they were placed on dry paper tissue to remove surface water and then immediately weighed. Five specimens were tested for each sample.

$$\text{Swelling degree} = (W_{wet} - W_{dry})/W_{dry} \times 100\% \quad (1)$$

The tensile properties of NFC–CS samples were measured using an MTS Tytron 250 Microforce testing workstation at room temperature according to ASTM D882 (2002) and Bourbon et al. (2011). Films were cut into strips (20 mm × 5 mm), and the gauge length was 10 mm. The crosshead speed was set at 5.0 mm/min. At least five measurements were carried out for each type of film.

3. Results and discussion

3.1. Optical properties of NFC–CS nanocomposites

NFC–CS nanocomposite films with a thickness of 0.1–0.15 μm containing various contents of NFC were prepared through solution casting from NFC aqueous suspension containing CS. The as-cast films were used for tests without any neutralizing treatments. The optical properties of the as-cast films were evaluated by measuring their transmittance in the range

215–800 nm, as shown in Fig. 1. They exhibit transmittances of 40% and higher at or above 300 nm. The percent transmittances at 300 nm, 400 nm, and 500 nm are tabulated in Table 1. The transmittance values of CS studied here are 86.6% at 400 nm and 90.5% at 500 nm, in good agreement with literature data (Fernandes et al., 2010; Fernandes et al., 2009; Larena and Cáceres, 2004). With increasing content of NFC, the percent transmittance decreases slowly and NFC–CS nanocomposite films show high transparency with NFC content up to 8 wt%. The transmittance decreases relatively quickly with NFC content more than 8 wt% compared to samples containing NFC below 8 wt%. As expected, there is some scattering and/or absorption from the NFC–CS interface in scales from nanometers to micrometers, resulting in a moderate loss transmission for nanocomposites. Nevertheless, the NFC–CS nanocomposite film still shows good transparency when the NFC content is 32 wt%. Both the photos of CS and CS32 (Fig. 2(a)) demonstrate high optical clarity of the films, with the text underneath clearly legible. The top surface of pure NFC film is shown in Fig. 2(b). It shows cellulose fibrils or their bundles have a width below 200 nm. From SEM micrograph of CS32 (Fig. 2(c)), the good dispersion of NFC in the CS matrix can be seen. These results indicate good compatibility between CS and NFC in the nanocomposite films that results in homogeneous and transparent materials.

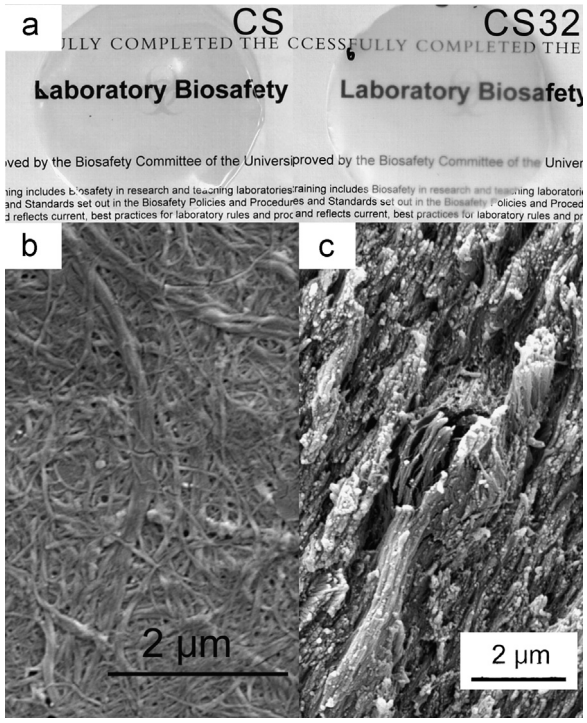

Fig. 2 – Photographs of CS and CS32 films (a), SEM images of top surface of NFC (b) and cross section of CS32 (c).

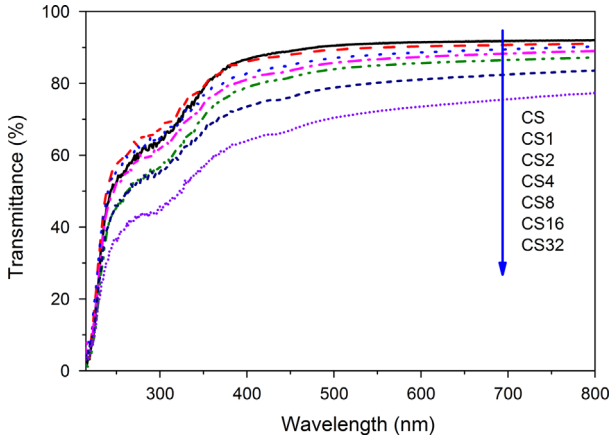

Fig. 1 – Transmittance UV–vis spectra of NFC–CS films scanned from 215 nm to 800 nm.

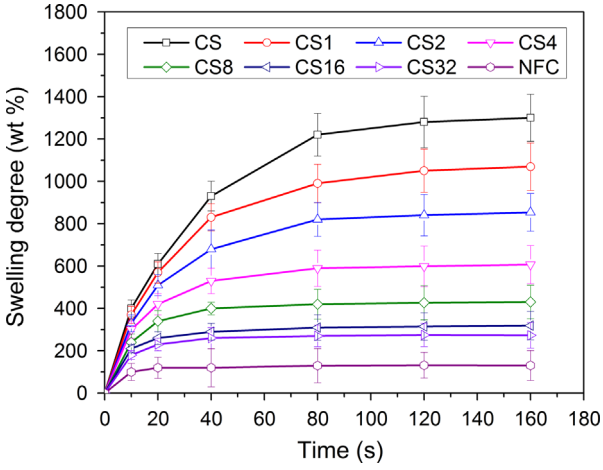

Fig. 3 – Swelling degree as a function of immersion time in distilled water for NFC–CS nanocomposites.

Table 1 – UV–vis transmittances of NFC–CS films at 300 nm, 400 nm, and 500 nm.

Sample	Transmittance (%)		
	300 nm	400 nm	500 nm
CS	64.2	86.6	90.5
CS1	66.9	86.0	89.3
CS2	64.7	82.7	87.0
CS4	61.1	81.1	85.7
CS8	56.4	78.9	83.9
CS16	55.1	73.4	78.8
CS32	45.7	64.0	70.3

3.2. *Swelling behavior of NFC–CS nanocomposites*

Experimental data for the swelling degree within distilled water for NFC–CS nanocomposite films are shown in Fig. 3. The data clearly show that all nanocomposite samples absorb water rapidly within the first 20 s and gradually reach the equilibrium within 160 s. The time needed to reach the equilibrium swelling degree is dependent on the content of NFC; it reduces with increasing NFC content from around 160 s for pure CS film to about 40 s for CS32 film and further to about 20 s for pure NFC film. Correspondingly, the equilibrium swelling degree also decreases with increasing content of NFC, from 1300% for CS to 270% for CS32, because of the

relatively low water absorption of NFC (130%). This suggests that the incorporation of NFC significantly reduces the equilibrium swelling degree of the CS matrix. The change of the equilibrium swelling degree can be understood by the effect of the restraining force in nanocomposites (Vervoort et al., 2005). The NFC network prevents the large dimensional change of CS, which results in a lower equilibrium swelling degree (Zrinyi et al., 1993).

The transportation of water through polymer composites depends on the chemical nature of the polymer and the filler, the filler dimensions, and polymer–filler interactions (Adhikary et al., 2008), which has been modeled by several researchers using Fick's second law, expressed as Eq. (2) (Asaoka and Hirano, 2003; Crank, 1975; Han et al., 1995; Santos et al., 2002).

$$\partial C/\partial t = D\partial^2 C/\partial x^2 \quad (2)$$

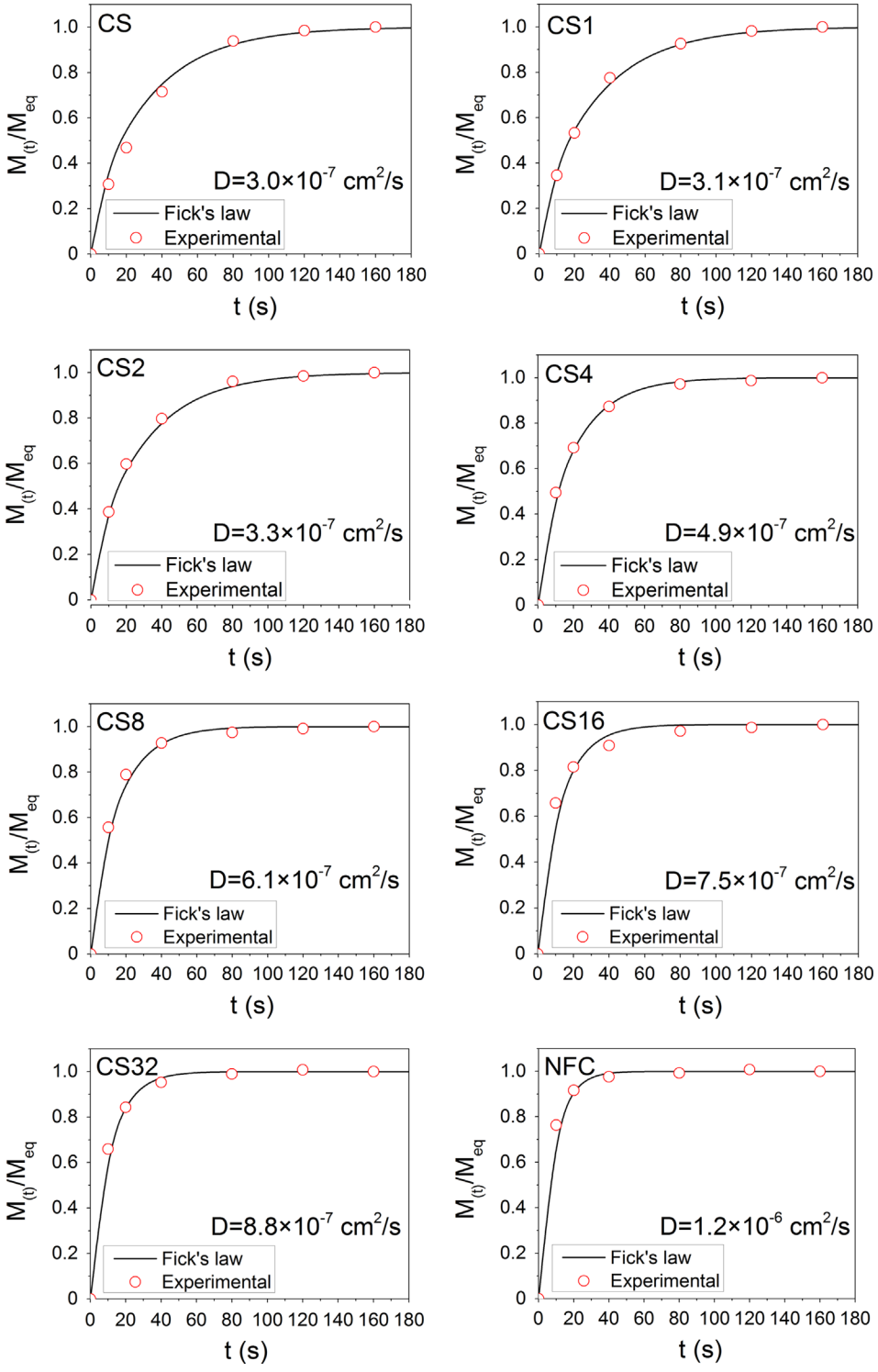

Fig. 4 – $M_{(t)}/M_{eq}$ as a function of time t for NFC–CS nanocomposite films.

Here, C denotes the concentration of the diffusing water at time t along the axis x. D is the diffusion coefficient. For a plane sheet geometry and if the initial concentration of water in the solid boundary is zero and the polymer is placed in an infinite bath of water, the solution is given by Eq. (3) (Crank, 1975).

$$M_{(t)}/M_{eq} = 1-(8/\pi^2)\sum_{m=0}^{\infty}\exp[-\pi^2(2m+1)^2Dt/L^2]/(2m+1)^2 \quad (3)$$

where L is the thickness of the specimen and $M_{(t)}$ and M_{eq} are the swelling degree of the specimen at times t and the equilibrium swelling degree, respectively. Fig. 4 shows the experimental values of $M_{(t)}/M_{eq}$ for NFC–CS nanocomposites, along with theoretical values of D predicted using Eq. (3). The diffusion of water into CS, NFC and NFC–CS nanocomposites follows Fick's law very closely in the whole swelling process, confirming that it can be used to adequately describe their swelling. The value of D estimated by Fick's law for the CS film here is 3.0×10^{-7} cm^2/s, which is in the range of 1.5×10^{-9}–3×10^{-5} cm^2/s for non-neutralized CS reported in previous literature (Lagarón and Fendler, 2009; Pereda et al., 2009). D for neutralized CS films is in the order of 4.1×10^{-9} cm^2/s (Tual et al., 2000). This indicates that the value of D for non-neutralized CS depends on the residual quantity of acetic acid, because of the protonation of chitosan (Nyström et al., 1999; Rinaudo et al., 1999). The estimated D for NFC film here is 1.2×10^{-6} cm^2/s, which is close to the literature value (2.18×10^{-6} cm^2/s) for cell-wall water in redwood sapwood at 26.5 °C (Araujo et al., 1993) and is in the order of 10^{-6}–10^{-7} cm^2/s reported for paper sheets (Perkins and Batchelor, 2012). Owing to the high diffusion coefficient of NFC, D is enhanced by up to 1.9 times from 3.0×10^{-7} cm^2/s for CS to 8.8×10^{-7} cm^2/s for CS32 in this case. The estimated values of D for NFC–CS nanocomposites lie between the data for NFC and CS, indicating they are reasonable. This phenomenon that an improved diffusion coefficient comes with depressed equilibrium swelling degrees was also observed in the swelling behavior of cross-linked chitosan reported in previous literature (Gonçalves et al., 2005).

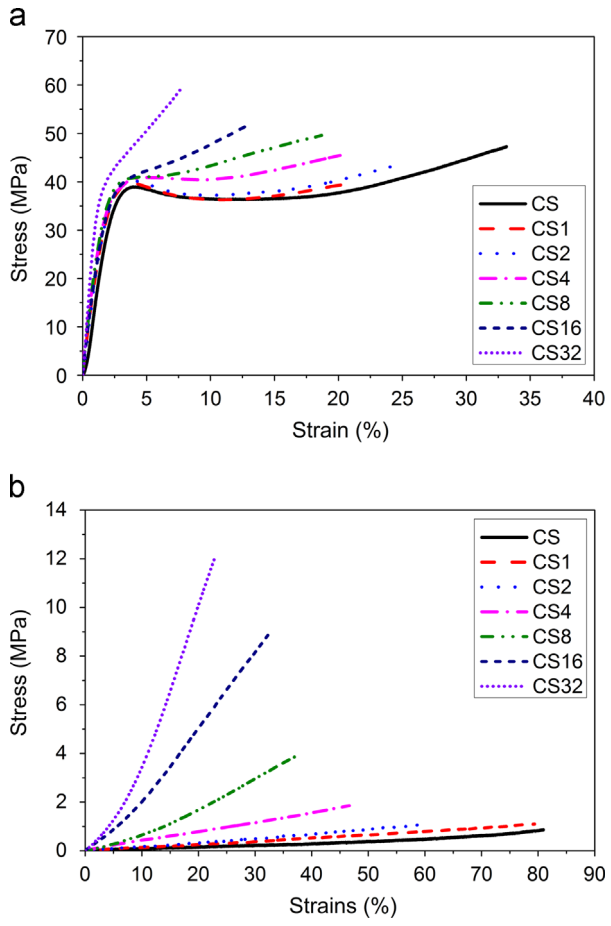

Fig. 5 – Representative tensile stress–strain curves for CS and NFC–CS nanocomposite films: dry (a) and wet (b).

3.3. *Mechanical properties of NFC–CS nanocomposites*

Fig. 5 shows representative tensile stress–strain curves of NFC–CS nanocomposites with varying NFC contents at dry and wet conditions and the tensile properties are summarized in Table 2. It can be seen that yield strength increases with increasing NFC content. The yield strength of CS8 is 5% higher than that of CS. For dry samples, ultimate tensile strength increases with increasing NFC content, but the values for the samples containing NFC below 8 wt% are lower than that of pristine CS. By combining stress–strain curves in Fig. 5(a) and the negative effect of the incorporation of NFC on the elongation at break (Table 2, column 5), it can be deduced that the low ultimate strength for samples containing NFC below 8 wt% is caused by the shortened elongation under stretching. Ultimate strengths of CS16 and CS32 are 12% and 25% larger than that of CS, respectively. Young's modulus is calculated from the initial linear region of

Table 2 – Tensile properties of NFC–CS nanocomposites.

Sample	Yield strength (MPa)	Ultimate strength (MPa)		Elongation at break (%)		Young's modulus (MPa)	
	Dry	Dry	Wet[a]	Dry	Wet[a]	Dry	Wet[a]
CS	38.9±16.5	46.5±14.9	0.9±0.6	36.5±7.1	81.2±11.2	1700±300	0.8±0.1
CS1	39.5±18.7	41.8±15.2	1.1±0.5	24.0±6.7	80.3±16.5	2100±500	1.3±0.4
CS2	40.1±12.6	42.6±16.1	1.2±0.6	22.1±6.1	61.5±10.3	2200±600	1.7±0.6
CS4	40.7±13.9	45.2±17.4	1.9±0.9	20.3±7.2	47.6±9.4	2000±600	3.9±0.9
CS8	40.9±19.1	49.9±15.8	3.9±1.8	18.2±6.8	37.3±7.9	2100±900	6.3±1.4
CS16	–	51.9±15.4	9.1±3.4	12.7±7.2	33.2±8.6	2300±500	18.0±4.0
CS32	–	58.3±16.2	12.1±2.2	7.6±3.5	23.1±5.7	3400±700	25.1±7.3

[a] Wet samples were obtained by immersion in water for 160 s to reach the equilibrium.

the tensile stress–strain curves. It increases with increasing NFC content, due to the reinforcement of NFC. Young's modulus for CS32 is improved by 100% in comparison with CS.

The tensile stress–strain curves obtained in wet conditions are shown in Fig. 5(b). The ultimate strength of CS immersed in distilled water for 160 s is 0.9 MPa (Table 2, column 4), which is much lower than the value for dry CS due to the plasticizing effect of water. The ultimate strength of NFC–CS nanocomposites immersed in distilled water for 160 s increases with increasing NFC content. The improvement of ultimate strength induced by NFC is much greater than that in dry conditions. For example, ultimate strength is improved by 9 and 12 times for wet CS16 and wet CS32 respectively, compared to the value for wet CS. This is because of the low swelling degree suppressed by NFC as well as the reinforcement effect of NFC, both originating from the high content of NFC. Similarly, Young's modulus of wet samples increases with increasing NFC content, with Young's modulus for wet CS32 being improved by 220% in comparison with wet CS. In contrast, the elongation at break for the wet samples decreases with increasing NFC content, which is of the same trend as in dry conditions. From SEM images of the fracture surface for CS4 (Fig. 6), it can be seen that the fracture surface of the wet sample is much coarser than that of the dry sample, confirming the improved ductility of the NFC–CS nanocomposite in the former.

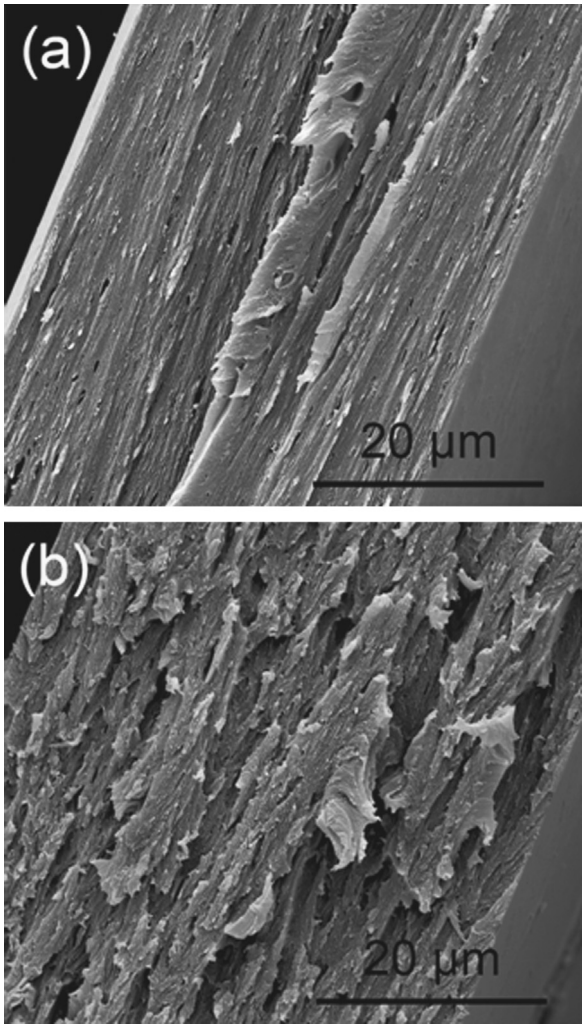

Fig. 6 – SEM images of the fracture surface of CS4 under dry (a) and wet (b) conditions.

NFC–CS nanocomposites have a similar architecture to the elastic tissue in skin which consists of superficial thin bundles of collagen microfibrils. The elasticity of wet NFC–CS nanocomposites is nonlinear and increases with increasing strain, as shown in Fig. 5(b), which is also like the nonlinear elasticity of human skin (Alexander and Cook, 1977). The initial modulus of wet NFC–CS nanocomposites is tunable in a broad range of 0.78–25 MPa and the elongation at break is in the range of 81–23%, by controlling the amount of NFC, which match well literature data of human skin (the initial stiffness reported as 0.1–2 MPa and 63% for failure stretch) (Annaidh et al., 2010; Manschot and Brakkee, 1986). The residual acetic acid on the nanocomposite film surface can be readily removed by washing the film with water or phosphate buffered saline solutions, which is a common process for handling biomaterials before they undergo cell culturing experiments, rendering no toxicity to the film. The appropriate mechanical properties of NFC–CS nanocomposite films, together with the excellent biocompatibility and biodegradability of NFC and CS and the high transparency, offer potential for the nanocomposites to be used as transparent edible films and coatings, artificial skin and wound dressings.

4. Conclusions

Highly transparent chitosan nanocomposite films reinforced with nanofibrillar cellulose were successfully prepared by solution casting. The high transparency indicated the excellent dispersion of NFC in the chitosan matrix. NFC suppressed the water uptake of CS; the equilibrium swelling degree of as-cast films decreased with increasing NFC content while the diffusion coefficient increased with increasing NFC content. The mechanical properties of NFC–CS nanocomposites were also dependent on the content of NFC. Under the dry conditions, the yield strength and Young's modulus of chitosan increased with increasing NFC content because of the reinforcement of NFC, while the elongation at break decreased. The improvements of ultimate strength and Young's modulus in wet samples were larger than those for dry samples. For example, ultimate strength was improved by 25% and 12 times for dry CS32 and wet CS32, respectively, compared to the values for dry and wet CS. This was attributed to the low swelling degree suppressed by NFC and the reinforcement effect of NFC. The mechanical behavior of wet NFC–CS nanocomposite films matched well those of human skin. Their prominent properties could be exploited for a number of applications, such as in artificial skin and wound dressings.

Acknowledgments

We thank the Irish Research Council for Science, Engineering & Technology and the University of Sheffield for financial

support. We also thank Professor Mohini Sain at University of Toronto for providing nanofibrillar cellulose.

REFERENCES

Adhikary, K.B., Pang, S., Staiger, M.P., 2008. Long-term moisture absorption and thickness swelling behaviour of recycled thermoplastics reinforced with Pinus radiata sawdust. Chem. Eng. J. 142, 190–198.

Agnihotri, S.A., Mallikarjuna, N.N., Aminabhavi, T.M., 2004. Recent advances on chitosan-based micro- and nanoparticles in drug delivery. J. Control. Release 100, 5–28.

Alexander, H., Cook, T.H., 1977. Accounting for natural tension in the mechanical testing of human skin. J. Invest. Dermatol. 69, 310–314.

Annaidh, A.N., Ottenio, M., Bruyère, K., Destrade, M., Gilchrist, M.D., 2010. Mechanical properties of excised human skin. In: Lim, C.T., Goh, J.C.H. (Eds.), 6th World Congress of Biomechanics (WCB 2010). Springer, Berlin Heidelberg, pp. 1000–1003.

Araujo, C.D., Mackay, A.L., Whittall, K.P., Hailey, J.R.T., 1993. A diffusion model for spin–spin relaxation of compartmentalized water in wood. J. Magn. Reson., Series B 101, 248–261.

Asaoka, K., Hirano, S., 2003. Diffusion coefficient of water through dental composite resin. Biomaterials 24, 975–979.

Azeez, A.A., Rhee, K.Y., Park, S.J., Kim, H.J., Jung, D.H., 2013. Application of cryomilling to enhance material properties of carbon nanotube reinforced chitosan nanocomposites. Compos. Part B: Eng. 50, 127–134.

Baheti, V., Militky, J., 2013. Reinforcement of wet milled jute nano/micro particles in polyvinyl alcohol films. Fibers Polym. 14, 133–137.

Bourbon, A.I., Pinheiro, A.C., Cerqueira, M.A., Rocha, C.M.R., Avides, M.C., Quintas, M.A.C., Vicente, A.A., 2011. Physico-chemical characterization of chitosan-based edible films incorporating bioactive compounds of different molecular weight. J. Food Eng. 106, 111–118.

Crank, J., 1975. The Mathematics of Diffusion. Oxford University Press, Oxford.

Crini, G., Badot, P.-M., 2008. Application of chitosan, a natural aminopolysaccharide, for dye removal from aqueous solutions by adsorption processes using batch studies: a review of recent literature. Prog. Polym. Sci. 33, 399–447.

Dahman, Y., Oktem, A.T., 2012. Optically transparent nanocomposites reinforced with modified biocellulose nanofibers. J. Appl. Polym. Sci. 126, E187–E195.

Dash, M., Chiellini, F., Ottenbrite, R.M., Chiellini, E., 2011. Chitosan—a versatile semi-synthetic polymer in biomedical applications. Prog. Polym. Sci. 36, 981–1014.

Fernandes, S.C.M., Freire, C.S.R., Silvestre, A.J.D., Pascoal Neto, C., Gandini, A., Berglund, L.A., Salmén, L., 2010. Transparent chitosan films reinforced with a high content of nanofibrillated cellulose. Carbohydr. Polym. 81, 394–401.

Fernandes, S.C.M., Oliveira, L., Freire, C.S.R., Silvestre, A.J.D., Neto, C.P., Gandini, A., Desbrieres, J., 2009. Novel transparent nanocomposite films based on chitosan and bacterial cellulose. Green Chem. 11, 2023–2029.

Gonçalves, V.L., Laranjeira, M.C.M., Fávere, V.T., Pedrosa, R.C., 2005. Effect of crosslinking agents on chitosan microspheres in controlled release of diclofenac sodium. Polímeros 15, 6–12.

Han, H., Gryte, C.C., Ree, M., 1995. Water diffusion and sorption in films of high-performance poly(4,4′-oxydiphenylene pyromellitimide): effects of humidity, imidization history and film thickness. Polymer 36, 1663–1672.

Hassan, M., Hassan, E., Oksman, K., 2011. Effect of pretreatment of bagasse fibers on the properties of chitosan/microfibrillated cellulose nanocomposites. J. Mater. Sci. 46, 1732–1740.

Hassan, M.L., Fadel, S.M., El-Wakil, N.A., Oksman, K., 2012. Chitosan/rice straw nanofibers nanocomposites: preparation, mechanical, and dynamic thermomechanical properties. J. Appl. Polym. Sci. 125, E216–E222.

Henriksson, M., Berglund, L.A., Isaksson, P., Lindstrom, T., Nishino, T., 2008. Cellulose nanopaper structures of high toughness. Biomacromolecules 9, 1579–1585.

Herrick, F.W., Casebier, R.L., Hamilton, J.K., Sandberg, K.R., 1983. Microfibrillated cellulose: morphology and accessibility. J. Appl. Polym. Sci. Appl. Polym. Symp. 37, 797–813.

Huang, H., Yuan, Q., Yang, X., 2004. Preparation and characterization of metal–chitosan nanocomposites. Colloids Surf. B: Biointerfaces 39, 31–37.

Jayakumar, R., Menon, D., Manzoor, K., Nair, S.V., Tamura, H., 2010. Biomedical applications of chitin and chitosan based nanomaterials—a short review. Carbohydr. Polym. 82, 227–232.

Khor, E., Lim, L.Y., 2003. Implantable applications of chitin and chitosan. Biomaterials 24, 2339–2349.

Kim, I.-Y., Seo, S.-J., Moon, H.-S., Yoo, M.-K., Park, I.-Y., Kim, B.-C., Cho, C.-S., 2008. Chitosan and its derivatives for tissue engineering applications. Biotechnol. Adv. 26, 1–21.

Krajewska, B., 2004. Application of chitin- and chitosan-based materials for enzyme immobilizations: a review. Enzyme Microb. Technol. 35, 126–139.

Lagarón, J.M., Fendler, A., 2009. High water barrier nanobiocomposites of methyl cellulose and chitosan for film and coating applications. J. Plast. Film Sheeting 25, 47–59.

Larena, A., Cáceres, D.A., 2004. Variability between chitosan membrane surface characteristics as function of its composition and environmental conditions. Appl. Surf. Sci. 238, 273–277.

Li, J., Chen, Y., Yin, Y., Yao, F., Yao, K., 2007. Modulation of nano-hydroxyapatite size via formation on chitosan–gelatin network film in situ. Biomaterials 28, 781–790.

Li, Q., Zhou, J., Zhang, L., 2009. Structure and properties of the nanocomposite films of chitosan reinforced with cellulose whiskers. J. Polym. Sci. Part B: Polym. Phys. 47, 1069–1077.

Manschot, J.F.M., Brakkee, A.J.M., 1986. The measurement and modelling of the mechanical properties of human skin in vivo —II. The model. J. Biomech. 19, 517–521.

Matsuo, M., Sawatari, C., Iwai, Y., Ozaki, F., 1990. Effect of orientation distribution and crystallinity on the measurement by X-ray diffraction of the crystal lattice moduli of cellulose I and II. Macromolecules 23, 3266–3275.

Mendez, J., Annamalai, P.K., Eichhorn, S.J., Rusli, R., Rowan, S.J., Foster, E.J., Weder, C., 2011. Bioinspired mechanically adaptive polymer nanocomposites with water-activated shape-memory effect. Macromolecules 44, 6827–6835.

Muzzarelli, R., 2009. Chitins and chitosans for the repair of wounded skin, nerve, cartilage and bone. Carbohydr. Polym. 76, 167–182.

Nakagaito, A.N., Yano, H., 2004. The effect of morphological changes from pulp fiber towards nano-scale fibrillated cellulose on the mechanical properties of high-strength plant fiber based composites. Appl. Phys. A 78, 547–552.

Nakagaito, A.N., Yano, H., 2005. Novel high-strength biocomposites based on microfibrillated cellulose having nano-order-unit web-like network structure. Appl. Phys. A 80, 155–159.

Nishino, T., Matsuda, I., Hirao, K., 2004. All-cellulose composite. Macromolecules 37, 7683–7687.

Nishiyama, Y., 2009. Structure and properties of the cellulose microfibril. J. Wood Sci. 55, 241–249.

Nogi, M., Iwamoto, S., Nakagaito, A.N., Yano, H., 2009. Optically transparent nanofiber paper. Adv. Mater. 21, 1595–1598.

Nyström, B., Kjøniksen, A.-L., Iversen, C., 1999. Characterization of association phenomena in aqueous systems of chitosan of different hydrophobicity. Adv. Colloid Interface Sci. 79, 81–103.
Oh, D.X., Hwang, D.S., 2013. A biomimetic chitosan composite with improved mechanical properties in wet conditions. Biotechnol. Prog. 29, 505–512.
Olsson, R.T., Azizi Samir, M.A.S., Salazar Alvarez, G., Belova, L., Strom, V., Berglund, L.A., Ikkala, O., Nogues, J., Gedde, U.W., 2010. Making flexible magnetic aerogels and stiff magnetic nanopaper using cellulose nanofibrils as templates. Nat. Nanotechnol. 5, 584–588.
Pääkkö, M., Ankerfors, M., Kosonen, H., Nykänen, A., Ahola, S., Österberg, M., Ruokolainen, J., Laine, J., Larsson, P.T., Ikkala, O., Lindström, T., 2007. Enzymatic hydrolysis combined with mechanical shearing and high-pressure homogenization for nanoscale cellulose fibrils and strong gels. Biomacromolecules 8, 1934–1941.
Pan, Y., Wu, T., Bao, H., Li, L., 2011. Green fabrication of chitosan films reinforced with parallel aligned graphene oxide. Carbohydr. Polym. 83, 1908–1915.
Pereda, M., Aranguren, M.I., Marcovich, N.E., 2009. Water vapor absorption and permeability of films based on chitosan and sodium caseinate. J. Appl. Polym. Sci. 111, 2777–2784.
Perkins, E.L., Batchelor, W.J., 2012. Water interaction in paper cellulose fibres as investigated by NMR pulsed field gradient. Carbohydr. Polym. 87, 361–367.
Pillai, C.K.S., Paul, W., Sharma, C.P., 2009. Chitin and chitosan polymers: chemistry, solubility and fiber formation. Prog. Polym. Sci. 34, 641–678.
Pitkänen, M., Honkalampi, U., Von Wright, A., Sneck, A., Hentze, H.P., Sievänen, J., Hiltunen, J., Hellén, E.K.O., 2010. Nanofibrillar cellulose—in vitro study of cytotoxic and genotoxic properties. In: Proceedibgs of the International Conference on Nanotechnology for the Forest Products Industry Otaniemi. Espoo, Finland.
Ravi Kumar, M.N.V., 2000. A review of chitin and chitosan applications. React. Funct. Polym. 46, 1–27.
Rinaudo, M., 2006. Chitin and chitosan: properties and applications. Prog. Polym. Sci. 31, 603–632.
Rinaudo, M., Pavlov, G., Desbrières, J., 1999. Influence of acetic acid concentration on the solubilization of chitosan. Polymer 40, 7029–7032.
Sakurada, I., Nukushina, Y., Ito, T., 1962. Experimental determination of the elastic modulus of crystalline regions in oriented polymers. J. Polym. Sci. 57, 651–660.
Santos, C., Clarke, R.L., Braden, M., Guitian, F., Davy, K.W.M., 2002. Water absorption characteristics of dental composites incorporating hydroxyapatite filler. Biomaterials 23, 1897–1904.
Sashiwa, H., Aiba, S.-i., 2004. Chemically modified chitin and chitosan as biomaterials. Prog. Polym. Sci. 29, 887–908.
Şenel, S., McClure, S.J., 2004. Potential applications of chitosan in veterinary medicine. Adv. Drug Deliv. Rev. 56, 1467–1480.
Shahidi, F., Arachchi, J.K.V., Jeon, Y.-J., 1999. Food applications of chitin and chitosans. Trends Food Sci. Technol. 10, 37–51.
Shimazaki, Y., Miyazaki, Y., Takezawa, Y., Nogi, M., Abe, K., Ifuku, S., Yano, H., 2007. Excellent thermal conductivity of transparent cellulose nanofiber/epoxy resin nanocomposites. Biomacromolecules 8, 2976–2978.
Siró, I., Plackett, D., 2010. Microfibrillated cellulose and new nanocomposite materials: a review. Cellulose 17, 459–494.
Tsourounaki, K., Bonné, M.J., Thielemans, W., Psillakis, E., Helton, M., McKee, A., Marken, F., 2008. Nanofibrillar cellulose–chitosan composite film electrodes: competitive binding of triclosan, $Fe(CN)_6^{3-/4-}$, and SDS surfactant. Electroanalysis 20, 2395–2402.
Tual, C., Espuche, E., Escoubes, M., Domard, A., 2000. Transport properties of chitosan membranes: influence of crosslinking. J. Polym. Sci. Part B: Polym. Phys. 38, 1521–1529.
Turbak, A.F., Snyder, F.W., Sandberg, K.R., 1983. Microfibrillated cellulose, a new cellulose product: properties, uses, and commercial potential.
Verma, D., Katti, K.S., Katti, D.R., Mohanty, B., 2008. Mechanical response and multilevel structure of biomimetic hydroxyapatite/polygalacturonic/chitosan nanocomposites. Mater. Sci. Eng.: C 28, 399–405.
Vervoort, S., Patlazhan, S., Weyts, J., Budtova, T., 2005. Solvent release from highly swollen gels under compression. Polymer 46, 121–127.
Wang, S.F., Shen, L., Tong, Y.J., Chen, L., Phang, I.Y., Lim, P.Q., Liu, T.X., 2005. Biopolymer chitosan/montmorillonite nanocomposites: preparation and characterization. Polym. Degrad. Stab. 90, 123–131.
Williams, C.K., Hillmyer, M.A., 2008. Polymers from renewable resources: a perspective for a special issue of polymer reviews. Polym. Rev. 48, 1–10.
Wu, Q., Henriksson, M., Liu, X., Berglund, L.A., 2007. A high strength nanocomposite based on microcrystalline cellulose and polyurethane. Biomacromolecules 8, 3687–3692.
Zrinyi, M., Rosta, J., Horkay, F., 1993. Studies on the swelling and shrinking kinetics of chemically crosslinked disk-shaped poly (vinyl acetate) gels. Macromolecules 26, 3097–3102.